Sensors and Actuators A 233 (2015) 32–41

Contents lists available at ScienceDirect

Sensors and Actuators A: Physical

journal homepage: www.elsevier.com/locate/sna

Siloxane-based thin films for biomimetic low-voltage dielectric actuators

Tino Töpper*, Florian Weiss, Bekim Osmani, Christian Bippes, Vanessa Leung, Bert Müller

University of Basel, Gewerbestrasse 14, Allschwil, CH 4123, Switzerland

ARTICLE INFO

Article history:
Received 10 December 2014
Received in revised form 15 June 2015
Accepted 15 June 2015
Available online 30 June 2015

Keywords:
Polydimethylsiloxane
Molecular beam deposition
AFM nanoindentation
Ultraviolet spectroscopy
Mid-infrared spectroscopy
Cantilever bending
Artificial muscle

ABSTRACT

Molecular beam deposition of siloxane-based polymer thin films was employed to realize single-layer dielectric elastomer actuators. With molecular weights of 6000 and 28,000 g/mol, vinyl-terminated polydimethylsiloxane (PDMS) was evaporated under high-vacuum conditions at crucible temperatures between 100 and 180 °C. Both deposition rate and realizable film thickness showed linear dependency with respect to the crucible temperature and were significantly higher for PDMS with lower molecular weight. Optimized growth conditions for 6000 g/mol were obtained at 180 °C with a deposition rate of (130 ± 5) nm per hour and a maximal film thickness of (530 ± 1) nm. Thermally induced polymerization was observed to limit the maximum accessible evaporation temperature for hydride-terminated PDMS above 180 °C and for vinyl-terminated PDMS above 230 °C. Ultraviolet (UV) light induced polymerization of vinyl-terminated PDMS was successfully established via radicalization at the functional vinyl end groups of the chains. Atomic force microscopy nanoindentation of the UV-polymerized network reveals that the oligomer chain length determines the elastic modulus of the polymer layer. Manufactured as asymmetric cantilever structures, the bending characteristic gave evidence that a 200 nm-thin film, activated in the voltage range between 1 and 12 V, maintains the actuation compared to a 4 μm-thick, spin-coated film, operated between 100 and 800 V. The force of the presented 200 nm-thin film cantilever actuator was about 10^{-4} N. This means that a multilayer actuator with more than 10^4 layers would reach forces comparable to natural muscles. Therefore, such nanostructures can qualify for medical applications for example to treat severe incontinence.

1. Introduction

Research on dielectric, electrically activated polymer (EAP) actuators for biomimetic implants focuses toward a significant reduction of the actuation voltages [1,2]. Micrometer-thick, silicone-based polymer films, prepared for example by spin-coating, require voltages in the range of several 100 V to a few kV to reach thickness strains of 25 to 48% [3,4]. Although the generation of high voltages through electromagnetic transformers is established, the limitations are large component size and often relatively low efficiency. Associated costs and potential health risks for medical device applications within the human body are further drawbacks. Therefore, one should either increase the dielectric constant of the polymer, for example by adding fillers in the elastomer network [5,6], or decrease the film thickness to reduce the operation voltage. Taking advantage of molecular beam deposition (MBD), we follow the pathway to reduce the film thickness to the sub-micrometer range. Compared with the well-established spin coating [7], solvents are not required. In order to reach the necessary actuation forces/pressures, however, stack actuators [8] have to be realized. This approach implies the reliable preparation of both polymer and stretchable electrode multilayers. Although MBD is known for excellent film homogeneity and relatively low defect densities, reliable MBD for polymer layers is challenging as heating in the crucible often causes dissociation to lower molecular weight components, pyrolysis, and even polymerization [9]. Such processes significantly modify evaporation rates and beam composition. These complex phenomena limits the evaporation temperature ranges typically to values between 150 and 450 °C and the deposition rates of the material to values below the desired range of about 1 μm/h or 1 monolayer/s. Nevertheless, once vacuum deposition of appropriate organic and electrode materials is available, one can prepare and characterize in situ film growth of multi-stack actuators under well-defined high-vacuum (HV) conditions.

* Corresponding author.

http://dx.doi.org/10.1016/j.sna.2015.06.014

It is hypothesized that MBD of vinyl-terminated polydimethylsiloxane (PDMS) with molecular weights M_w of 6000 and 28,000 g/mol allows for the preparation of low-voltage DEAs under HV conditions. We know that siloxane-based polymers are dielectric elastomers in actuator configurations because of their elasticity and dielectric behavior. Strain levels of 30 to 40% were reached [10]. Especially the millisecond response and the acceptance as a biocompatible material for applications within the human body make silicone suitable for biomimetic applications in artificial muscles [10,11].

Cross-linking of PDMS is achievable through the presence of functional groups either at the chain end or in the form of a copolymer. Covalent bonding can be realized either by heat-induced curing using a catalyst [12] or applying ultra-violet radiation to force the photo-initiated reaction of radicals [13,14]. Mid-infrared (MIR)-spectroscopy, for example, can support the analysis of polymerization in vinyl-terminated PDMS under continuous illumination by means of a deuterium broadband lamp, avoiding any use of cross-linkers or catalysts.

To characterize the performance of planar EAP actuators one can place them on a rectangular cantilever and measure the bending as a function of the applied voltage. Recently, experimental results of such a cantilever bending system [15] were published. Here a 200 nm-thin silicone film was embedded between two Au electrodes each 10 nm-thin. This EAP actuator was placed on a 25 μm-thick polyetheretherketone (PEEK) cantilever to obtain an asymmetric structure, which notably bends through the application of a voltage as small as a few volts. The cantilever bending approach is known from atomic force microscopy and similar methods to be extremely sensitive, see e.g. [16]. Therefore, this approach has also been applied for the current study.

It can reasonably be expected that low-voltage DEAs prepared by means of biocompatible materials with intrinsic properties, which include millisecond response and remarkable energy efficiency [10], will not only become parts of medical implants but find applications in a wide variety of other fields.

2. Materials and methods

2.1. Silicones used

The study on thermal evaporation is based on vinyl-terminated dimethylsiloxane DMS-V21 (Gelest Inc., Morrisville, PA, USA), vinyl-dimethylsiloxane copolymer AB116647 (abcr GmbH, Karlsruhe, Germany) and hydride-terminated hydride-dimethylsiloxane copolymer HMS-H271 (Gelest Inc., Morrisville, PA, USA). Elastosil 745 A/B (Wacker Chemie AG, München, Germany) is solely used for spin coating of micrometer-thick films.

2.2. Thermal characterization of PDMS

The characterization of thermal degradation was carried out with thermal gravimetric analysis (TGA) using a TGA/SDTA851e system (Mettler Toledo, Greifensee, Switzerland). The data were acquired with a heating rate of 10 K per minute under nitrogen atmosphere for PDMS terminated with hydride and vinyl groups. The temperature at which thermally induced crosslinking occurs was determined by heating micrometer-thin films with a rate of 5 K per hour, starting from 150 °C under atmospheric conditions.

2.3. Thermal evaporation of PDMS

The deposition experiments were carried out under high-vacuum conditions. After bake-out at a temperature of 120 °C for two hours, a base pressure of 10^{-8} mbar was achieved using a Agilent SH-110 dry scroll pump (Swissvacuum Technologies SA, Marin-Epagnier, Switzerland) with a pumping speed of 110 l/min in combination with Agilent V-81-M turbo pump (Swissvacuum Technologies SA, Marin-Epagnier, Switzerland) with a pumping speed of 77 l/s for N_2 at a rotation frequency of 1350 Hz. We utilized a low temperature effusion cell (Dr. Eberl MBE Komponenten GmbH, Weil der Stadt, Germany) with precise regulation and high temperature stability in order to realize a homogeneous temperature distribution inside the crucible (NTEZ crucible with a volume of 2 cm^3). The temperature ramp of the evaporator was adjusted to a heating rate of 10 K per minute. When the shutter of the evaporator was opened a rise of the vapor pressure was detected to 1×10^{-6} mbar and up to 5×10^{-6} mbar at 120 °C and 180 °C source temperature, respectively. The pressure was detected with a FRG-700 Varian inverted Magneton Pirani Gauge (Swissvacuum Technologies SA, Marin-Epagnier, Switzerland) in front of the turbo pump, at a distance of 600 mm to the evaporator. The substrate was placed 300 mm in front of the evaporation source. A quartz crystal microbalance (LewVac, Ote Hall Farm, Burgess Hill, UK) served for the film thickness measurement.

2.4. Crosslinking of poly-dimethylsiloxane (PDMS)

Photodecomposition of Si-vinyl bonds occurs as a result of direct UV radiation with a wavelength below 300 nm [17]. To obtain the radicalization wavelength of the Si-vinyl bonds, a UV–vis measurement was performed with an Agilent 8453 Spectrometer (Agilent Technologies, Basel, Switzerland). The solvent hexane (HPLC grade, Fischer Scientific, Wohlen, Switzerland) was utilized.

The UV radicalization was realized with a deuterium D2 broadband UV lamp (Yuyu Lightning, China) covering a spectral range between 180 and 450 nm with maximum intensity at a wavelength of 210 nm.

Mid-infrared (MIR) spectroscopy with a Varian 670-IR spectrometer (Varian Inc., Santa Clara, USA) was used to investigate the resulting polymer network by analyzing the absorption bands of bond-vibrations from 600 to 4000 cm^{-1} with steps of 4 cm^{-1}.

2.5. Nanoindentation of PDMS cross-linked networks

The nanomechanical properties of the deposited polymers were quantified using the FlexAFM ARTIDIS system (Nanosurf AG, Liestal, Switzerland). The nominal spring constant of the cantilevers (CONTSCR, Nanosensors, Neuchatel, Switzerland) was determined to be 0.2 N/m using the Sader method [18]. The ARTIDIS system allows systematic sampling at selected points of interest. The size of each spot was either 15×15 μm^2 or 20×20 μm^2. Each spot was overlaid with a 64×64 points array. The array defines the locations of the 4096 nanoindentation tests. The FlexAFM ARTIDIS automatically acquired the data and generated a stiffness map and histogram for each spot. The power law method by Oliver & Pharr [19] was used to calculate the Young's modulus. The CONTSCR-cantilever tip radius was 7 nm. The approach was done with a speed of 6 μm/s while the measurements were taken at a force setpoint of 4 nN.

2.6. Preparation and mechanical characterization of asymmetric EAP structures

The polymer films, either grown by MBD (see Section 2.3) with a thickness of 200 nm or spin-coated (Spincoater WS-400B-6NPP, Laurell Technologies, North Wales, USA) with a thickness of 4 μm (Elastosil A/B at 3000 rpm for 150 s, heat cured for 2 h at 120 °C), were embedded between two 10 nm sputtered Au-electrodes (Magnetron sputter system, Balzers Union SCD040,

Lichtenstein) and placed on a 25 μm polyetheretherketone PEEK substrate (Aptiv 2000, Vitrex, Lancashire, UK). The related sputtering conditions corresponded to 0.05 mbar Ar-atmosphere and a constant working current of 30 mA. The thickness of the Au electrodes was 10 nm, determined by a calibration curve plotting time versus thickness measured using a quartz crystal microbalance (QSG 301, Balzers, Lichtenstein). To get contact access to the lower electrode the grown PDMS layer was dissolved and washed off partially by submerging the structure into ethyl acetate. On the growth of an adhesion layer between PEEK and Au or PDMS and Au was renounced to simplify the actuation characterization. Nevertheless recently published results indicate that the conductivity as well as the adhesion of a 10 nm-thin Au electrode to the polymer is sufficiently high enough to follow strains as large as 20% [20]. The thickness of the polymer layer after MBD or spin-coating and following polymerisation was determined using 3D laser microscopy (Keyence VK-X200, Keyence International, Belgium) with a spatial resolution of 0.5 nm in z-direction. Finally, this stack was cut into asymmetric cantilever structures (cf. Fig. 8).

With the advantage of no severe geometric restrictions, the cantilever beam deflection method has shown the potential to characterize the mechanics of thin films on a substrate [21–23], and cells on a cantilever [24] or even on whole asymmetric EAP structures [25–27]. Therefore, we applied this method to characterize EAP films by means of electrical actuation. A detailed description of the utilized apparatus can be found in literature [15,26]. When a voltage U is applied between the two electrodes, an electrostatic pressure p leads to a strain in the vertical direction S_z (Eq. (1)), which is then, due to the incompressibility of the polymer network, equally translated into a strain in horizontal directions S_x and S_y.

$$S_x = \frac{1}{2}S_z = -\frac{p}{2E} = -\frac{1}{2E}\varepsilon_r\varepsilon_0\left(\frac{U}{h_f}\right)^2 \quad (1)$$

This strain in the horizontal direction leads to a surface stress between the EAP film with thickness h_f and the PEEK-substrate, resulting in a torque that bends the entire EAP-cantilever structure. The bending can be detected by the deflection d of a reflected laser beam (660 nm Streamline diode laser, Laser2000, Germany) on a position sensitive detector (PSD, Spoton Laser2000) (see Fig. 4). According to Stoney [28]

$$S_x = \frac{E_s h_s^2}{6(1-\nu_s)h_f} \times \frac{d}{LD} \quad (2)$$

the strain S_x between the surfaces is proportional to the displacement d, which is dependent on the substrate properties (elastic modulus E_s thickness h_s). Merging Eqs. (1) and (2) it becomes clear that one can expect a quadratic dependence between the applied voltage U and the displacement d. The ratio between displacement d, cantilever length L, and the distance between the cantilever and the detector D can otherwise be described by the inverse of the bending radius R with $d/LD = 1/R$.

3. Results

3.1. Thermal characterization of PDMS

The thermal gravimetric analysis of the PDMS showed that the temperature onset of molecular weight loss $T_{\text{weight-loss}}$ is, with a value of 450 °C ± 20 K, 200 K lower for hydride-terminated (HMS-H271) than for the vinyl-terminated polymers (DMS-V21 and AB116647). In addition, we observed that hydride-terminated PDMS started to form cross-linked networks at temperatures above 180 °C ± 5 K, whereas vinyl-terminated PDMS required temperatures of 230 °C ± 5 K to form cross-linked networks under ambient conditions.

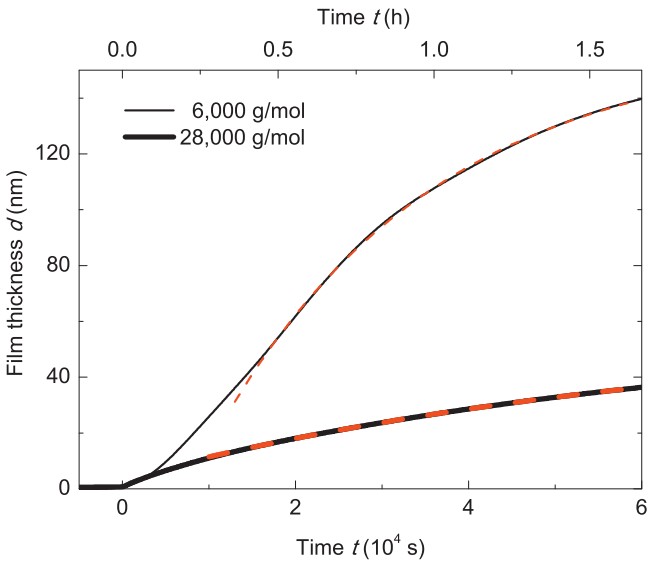

Fig. 1. Temporal behavior of molecular beam deposition of PDMS with molecular weights of 6000 (thin line) and 28,000 g/mol (thick line) at a source temperature of 120 °C and a background pressure of 1×10^{-6} mbar. Eq. (3) describes the experimentally observed time dependence as the fits (dashed lines) of the polymers with the molecular weights of 6000 g/mol ($d_{max} = (160.0 \pm 0.5)$ nm, $\tau = (2.52 \pm 0.01) \times 10^4$ s) and of 28,000 g/mol ($d_{max} = (58.0 \pm 0.2)$ nm, $\tau = (6.56 \pm 0.03) \times 10^4$ s), as indicated.

3.2. Thermal evaporation of PDMS

Figs. 1 and 2 demonstrate that the selected polymers can be evaporated under high-vacuum conditions to fabricate nanometer-thin polymer films. Due to the higher thermal stability of the vinyl-terminated PDMS, detailed investigations of MBD growth for DMS-V21 and AB116647 were gathered. At a source temperature of 120 °C in the time frame up to 10^4 s, a linear growth behavior for both polymers was observed. Eq. (3) below shows that the growth rate, related to the particle flux dd/dt = $j(T)$, is proportional to the

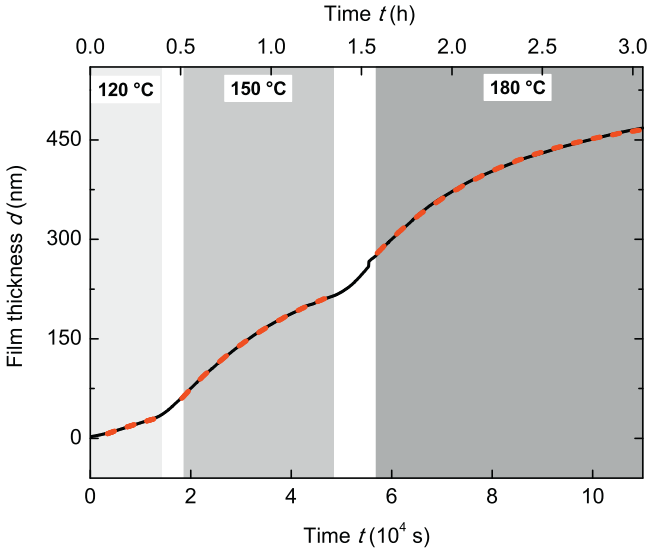

Fig. 2. The time dependence of the evaporation rate can be adjusted by the choice of the evaporation temperature. The representative graph for the molecular beam deposition of PDMS with a molecular weight of 6000 g/mol (DMS-V21) follows the behavior given by Eq. (3) at each of the source temperatures given. The time constant increases from (6.0 ± 0.3) via (8.6 ± 0.2) to (10.4 ± 0.1) × 10^4 s and the film thickness at infinite time reaches (95 ± 5), (280 ± 1), and (530 ± 1) nm, respectively.

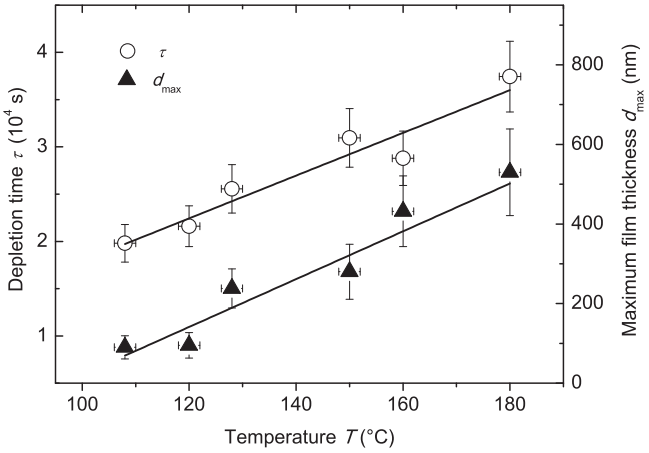

Fig. 3. The temperature dependences of the asymptotic film thickness d_{max} and the fitted time constants τ exhibit a linear behavior for the vinyl-terminated PDMS with a molecular weight of 6000 g/mol. One can take advantage from this behavior and select the optimized source temperature to reach the desired film thickness within the available period of time.

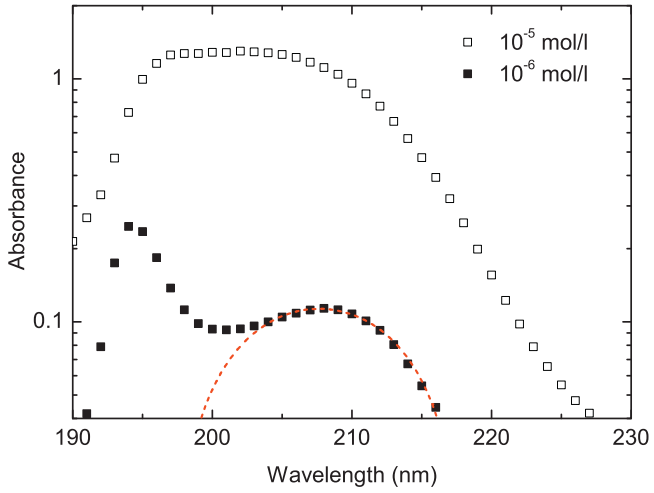

Fig. 4. Ultra-violet spectroscopy of the vinyl-terminated polymer AB116647, diluted in hexane to 10^{-5} and 10^{-6} mol/l. The $\pi - \pi^*$ transition of the vinyl double bond at (207.7 ± 0.1) nm was determined with a Gaussian fit using a solvent cut-off at the wavelength of (194.5 ± 0.1) nm.

equilibrium vapor pressure $p(T)$ and inversely proportional to the mass m of the molecules [29]:

$$j(T) = \frac{p(T)}{\sqrt{2\pi mkT}}. \quad (3)$$

The equation contains the Boltzmann constant k. During evaporation of the two polymers at the source temperature of 120 °C the background pressure was 10^{-6} mbar. The relation between the growth rates of the polymers with molecular weights of 6000 and 28,000 g/mol is therefore determined by the ratio of the square roots of the molecular weights, i. e. about 2.2. Experimentally we obtained growth rates of (130 ± 5) and (35 ± 2) nm per hour, respectively, which corresponds to a ratio of 3.7.

For evaporation times above 10^4 s we observed a deviation from the linear behavior. The growth rates became smaller and smaller. The acquired behavior can be described by the following equation:

$$d(t) = d_{max}\left[1 - \exp\left(-\frac{t}{\tau}\right)\right]. \quad (4)$$

For the source temperature of 120 °C we have fitted the two parameters, i.e. the asymptotic film thickness d_{max} and the time constant τ. Fig. 1 demonstrates that the polymer with lower molecular weight has a 2.6 smaller time constant than the PDMS with the larger molecular weight. The ratio of the maximal film thicknesses is found to be about 2.8.

The data of Fig. 1 show that using the present experimental setup, the polymer DMS-V21, and a source temperature of 120 °C one cannot realize films with a thickness above 160 nm. Fig. 2 presents our attempts for the polymer DMS-V21 to increase the maximal film thickness by applying higher source temperatures, i.e. 150 and 180 °C. This deposition experiment with a lower filling level of the source led to maximal film thicknesses of (95 ± 5), (280 ± 1), and (530 ± 1) nm, respectively. The related time constants also significantly increased from (6.0 ± 0.3) via (8.6 ± 0.2) to (10.4 ± 0.1) 10^4 s.

Fig. 3 demonstrates that the asymptotic film thickness and the related time constants linearly depend on the source temperature from 110 to 180 °C. The asymptotic film thickness as a function of the source temperature is described using the linear fit $d_{max}(T) = (6.0 \pm 1.1)\,\text{nm/K} \times T - (580 \pm 130)$ nm. The time constant follows a similar behavior: $\tau(T) = (226 \pm 31)\,\text{s/K} \times T - (470 \pm 40)$ s. The error bars of the fit parameters not only contain statistical errors derived from the fitted data but also reasonable estimates of the systematic errors. The measured data and the related linear fits displayed in Fig. 3 lead to the conclusion that at a source temperature below 100 °C, one does not obtain any meaningful film thickness. In general, deposition rates as high as 1 μm per hour are desired, corresponding to source temperatures above 180 °C. At source temperatures between 180 and 200 °C, however, we observed boiling retardation of the polymer DMS-V21 within the crucible associated with spitting of polymer material onto the substrate, although the evaporation source is known for homogenous temperature distribution.

3.3. Crosslinking of poly-dimethylsiloxane (PDMS)

Fig. 4 displays the absorbance of the AB116647 polymer film for wavelengths between 190 and 230 nm (ultra-violet spectroscopy). The dilution in hexane was adjusted to 10^{-6} mol/l to discriminate between the absorption peaks of the vinyl group and the solvent (see Fig. 4). Based on a Gaussian fit, one obtains the wavelength of the π–π^* transition of the vinyl double bond. It corresponds to (207.7 ± 0.1) nm.

The spectrum of the deuterium lamp thus covers the wavelength for activating the cleavage of the vinyl double bonds. Applied for a period of three hours, the polymer thin film received an energy density of $(3000 \pm 100)\,\text{W/m}^2$. The irradiance at the wavelength of 207.7 nm at a distance of 0.2 m was measured to be $(3.0 \pm 0.1)\,\text{mW/m}^2$ per nm.

Mid-infrared (MIR) spectroscopy data, as presented in Fig. 5, served for the investigation of modifications in the polymer owing to treatment with ultra-violet light. The data given in Fig. 5(a) show the absorption bands of vinyl ($SiCH{=}CH_2$) vibrations at the wavenumbers of 1590 cm^{-1}, 1410 cm^{-1}, and 960 cm^{-1}, as well as of the C—H bond vibration at the wavenumber of 3060 cm^{-1} as known from the literature [30].

The spectroscopy data of Fig. 5(b) include the Si—O vibration band at the wavenumber of 1065 cm^{-1} and the $SiCH_2$—CH_2Si vibrations around a wavenumber of 1130 cm^{-1} [30]. The absorbance of the polymer film before and after the UV irradiation have been normalized for the absorption band at the wavenumber of 1065 cm^{-1}, since the Si—O bonds are the most stable ones in the silicone chains. Table 1 of Ref. [31] contains the related dissociation energy, which corresponds to a radicalization wavelength of 155 nm. This wavelength is well below the ones generated by the lamp used.

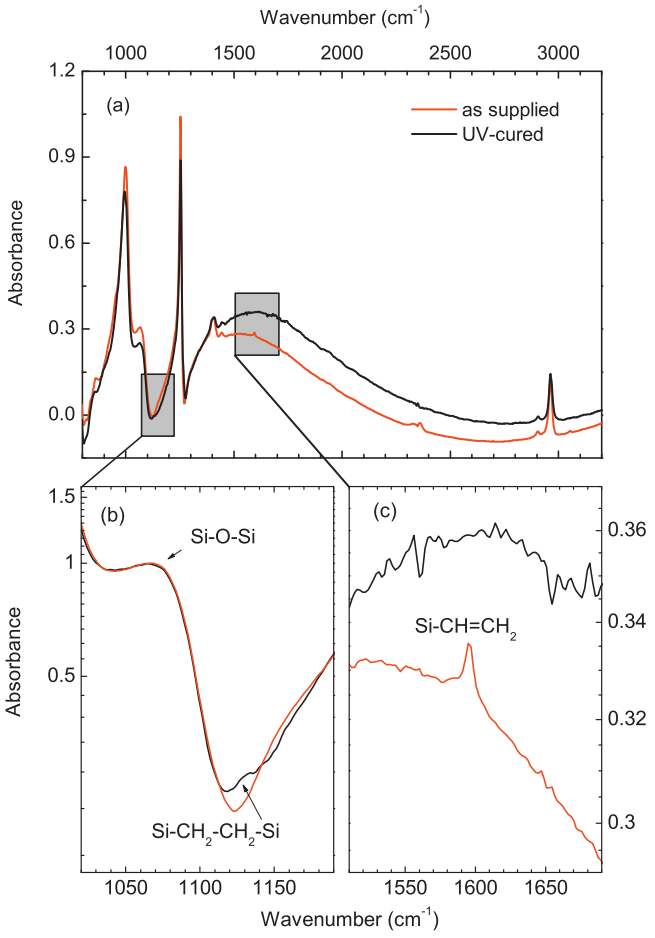

Fig. 5. Mid-infrared spectroscopy of the vinyl-terminated polymer DMS-V21: (a) The absorbance of the polymer as supplied corresponds to the red-colored data, the data in black are the absorbance values of the ultra-violet-cured thin film. (b) The data within the selected spectral range verify the occurrence of the absorption band around a wavenumber of 1130 cm^{-1} attributed to $SiCH_2$—CH_2Si vibrations. The absorbance was normalized according to the Si—O—Si vibration band at the wavenumber of 1065 cm^{-1} a feature assumed to be unaffected by the applied radiation. (c) The change of the vinyl vibration ($SiCH{=}CH_2$) at the wavenumber of 1590 cm^{-1} after the treatment is obvious. (For interpretation of the references to colour in this figure legend, the reader is referred to the web version of this article.)

Therefore, the spectroscopy data of Fig. 5(b) clearly indicate that a significant number of $SiCH_2$—CH_2Si bonds have been formed as the result of the UV treatment. At the wavenumber of 1130 cm^{-1} the absorbance increased from 0.22 to 0.26.

As exemplarily demonstrated for a wavenumber of 1590 cm^{-1} in Fig. 5(c), the peaks related to the vinyl bonds of the polymer before the UV treatment disappear after such a treatment.

3.4. Young's modulus determination of siloxane films

The frequency of the 4096 measured elastic moduli follows a Gaussian distribution for both the spin-coated and the evaporated DMS-V21 films. After UV-treatment, the spin-coated, 4 μm-thin polymer had an average elastic modulus of (480.9 ± 0.2) kPa with a half width of (16.2 ± 0.2) kPa, whereas the 200 nm-thin film prepared by molecular beam deposition gave rise to an average elastic modulus of (1685.8 ± 1.4) kPa with a half width of (187.5 ± 2.8) kPa. This means that the thin film prepared by evaporation at a source temperature of 120 °C is 3.5 times stiffer than the spin-coated microstructure.

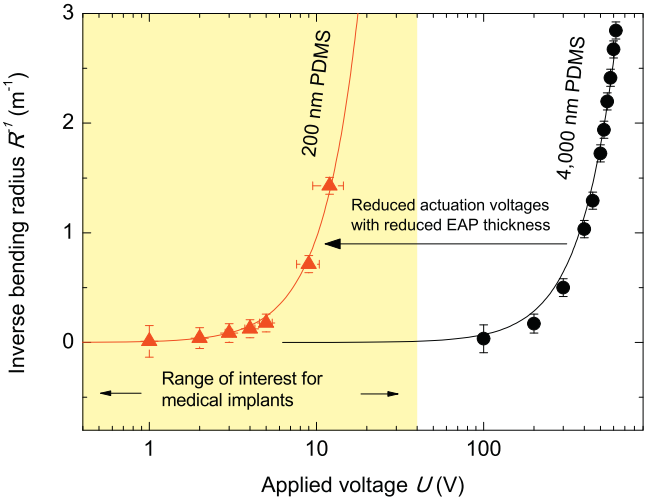

Fig. 6. The application of a voltage to the EAP micro- and nano-structures placed on 25 μm-thick PEEK substrates results in bending radii that follow the predicted quadratic behavior (fits represented by the full lines). The 200 nm-thin PDMS actuator demonstrated the aimed-for actuation efficiency within the medically relevant range of voltages for the realization of artificial muscles.

3.5. Bending of the asymmetric, dielectric actuators

Fig. 6 represents selected experimental data that follow the characteristic quadratic behavior predicted from Eq. (1). The full lines are the related fits. The currently state-of-the-art, 4 μm-thick, spin-coated, Elastosil A/B based actuators need voltages as high as several hundred volts to reach the desired deformation or stress-strain transfer (see Fig. 6). The 200 nm-thin, DMS-V21-based actuators (red triangles) prepared by molecular beam deposition at an evaporation temperature of 150 °C and subsequent UV-treatment actuates at voltages as low as a few volts and hence can become the basis of artificial muscles within the human body. It should be noted that the breakdown voltages corresponded to (60 ± 6) V/μm for the 200 nm-thin DMS-V21 polymer and (120 ± 12) V/μm for the 4 μm-thick Elastosil film. The maximal detected curvature of the cantilevers before breakdown was (2.67 ± 0.2) m^{-1} for the 4 μm-thick cantilever actuator applying a voltage of 500 V and (1.43 ± 0.1) m^{-1} for the 200 nm-thin cantilever actuator using a voltage of 12 V. The corresponding driving forces, applied at the cross-sectional area of the polymer film, are (5.9 ± 0.7) 10^{-3} N for the 4 μm-thick and (6.9 ± 1.2) 10^{-5} N for the 200 nm-thin cantilever actuator, respectively. For the horizontally mounted cantilever the curvature was calibrated based on the gravitational force. For the 4 μm-thick actuator a curvature of (1.41 ± 0.22) m^{-1} was detected. For the 200 nm-thin actuator the curvature corresponded to (1.25 ± 0.19) m^{-1}.

4. Discussion

PDMS is known for its resistance to environmental degradation induced by oxygen, ozone, and sunlight [6]. Furthermore, kinetics studies of thermal degradation have shown that the thermal stability of $(CH_3)_3Si$ end-blocked PDMS is present up to a temperature of 339 °C under ambient conditions [32]. The thermal treatment of terminated PDMS, however, does exhibit reduced thresholds of thermally induced cross-linking in air. This behavior

is related to the higher thermal stability of the $SiCH{=}CH_2$ double bond compared to the Si—H bond. Either placed at the end or in the middle of the polymer chain, the $SiCH{=}CH_2SiCH{=}CH_2$ bonds have an enthalpy of (690 ± 4) kJ/mol (see Table 4.11 of Ref. [33]). Alternatively, to radicalize the vinyl group, dissociation energies of (435 ± 21) kJ/mol for $SiC \rightarrow Si + C$ [34] and of (424 ± 1) kJ/mol for $CH_2 \rightarrow CH + H$ [33] have been reported. The dissociation energy of the Si—H bonds is with an amount of (377 ± 13) kJ/mol significantly lower [34]. Due to the highest dissociation energy of (462 ± 1) kJ/mol for the methyl side groups (see Table 4.11 of Ref. [33]), the thermal stability of PDMS is given by the termination of the siloxane chain. Therefore, the lower temperatures for Si—H compared to Si-vinyl bonds have to be exceeded so that bond cleavage and cross-linking do occur. This coincides with the fact that oxidation rates during thermal treatment of Si—H groups were found to be higher than the rates for the Si-vinyl groups [17,35]. The enhanced thermal stability of vinyl-terminated PDMS enables the use of higher evaporation temperatures and hence complies more to the demand for high evaporation rates than hydride-terminated PDMS. Israeli et al. have shown that the termination with phenyl groups improves the thermal stability of PDMS even further [36].

Consequently, the thermal evaporation of the PDMS has constrictions owing to the thermal stability of the polymer chains. Above the temperature range at which the PDMS is stable, the physical and chemical properties change associated with the shift of the molecular weight distribution [9]. The result depends on the concurrent rates of the decay and chain-linking processes within the evaporator. For evaporation temperatures well below thermal instability one observes a constant growth rate, which only depends on the source temperature. We observed this behavior only for the polymer with a low molecular weight of 6000 g/mol and within a restricted period of time. Subsequently, we have found an asymptotic decrease of the growth rates that limits the film thickness to a maximal value given by the choice of the source temperature. In general, time-dependent growth processes with N particles are described by a rate equation, often simply a differential equation of first order:

$$\frac{d^2N(t,T)}{dtdT} + \frac{1}{\tau}N(t,T) = 0. \quad (5)$$

Under static temperature conditions of the evaporation source, which we can reasonably assume, integration over time leads to the exponential behavior of $N(t)$ with the number of particles near the surface of the evaporation material N_s and the number of particles in the evaporation material N_c.

$$N(t) = N_s + N_c \exp\left(-\frac{t}{\tau}\right). \quad (6)$$

At a source temperature below 180 °C only molecules with a molecular weight much lower than the mean value and which are in the surface region of the evaporation material can leave the source. We hypothesize that the diffusion of the molecules does not compensate for the molecule's loss as the result of evaporation.

Thus, after the depletion of the particles with a relatively low molecular weight localized near the surface of the evaporation material, the diffusion rate within the polymer, characterized by the time constant τ, dominates the growth behavior. The diffusion rate of polymers between bulk and surface region, described by their viscosity, is inversely proportional to the molecular weight; in other words the surface depletion decreases with lower molecular weight. The evaporation rate, according to Eq. (3), is also inversely proportional to the molecular weight, thus we expect that the low molecular weight polymers have been evaporated faster. The ratio of the growth rates has been 3.7 times higher for the polymer with molecular weight of 6000 g/mol compared to 28,000 g/mol. The time constant for surface depletion, however, was found to be 2.6 smaller for the polymer with molecular weight of 6000 g/mol compared to 28,000 g/mol. Therefore, we conclude that the diffusion rate within the reservoir of polymer with molecular weight of 6000 g/mol is only 1.4 times higher compared to the polymer with molecular weight of 28,000 g/mol.

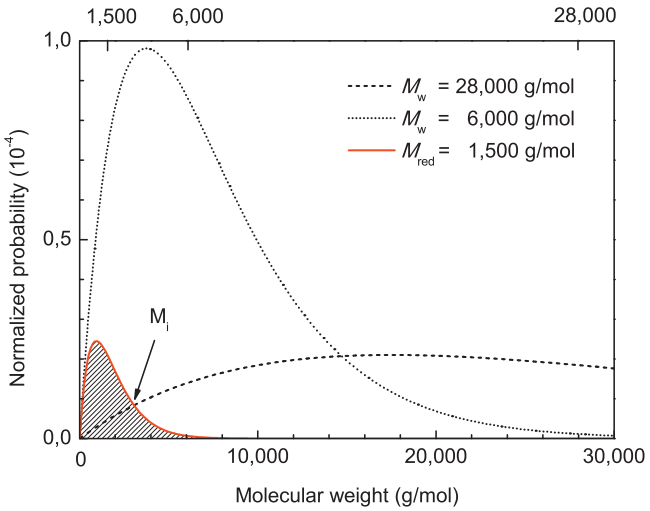

Fig. 7. The Flory distributions with average molecular weights of 28,000 g/mol (dashed line) and 6000 g/mol (dotted line) are shown. The schematic representation of evaporation probability of the polymer with nominal molecular weight of 6000 g/mol at a crucible temperature of 120 °C (red graph) demonstrates a preferential evaporation of low molecular weight oligomers with reduced average molecular weight of 1500 g/mol. The evaporation probability for polymers with nominal molecular weight of 28,000 g/mol is described by the overlap of MWD_{28000} with the reduced MWD_{1500}. The reduced MWD_{1500} can be found when the ratio of determined maximum film thicknesses of 2.6 is assigned to equal the ratio of integrals over the two shifted MWDs of the supplied polymers (see Eq. (7)). (For interpretation of the references to colour in this figure legend, the reader is referred to the web version of this article.)

The discrepancy factor of 2.6 between the experimentally obtained maximal film thicknesses can be explained by considering the polydispersity of the evaporation material. The polymers we were supplied with have molecular weight distributions (MWD), which might be described according to the Flory distribution [37]. The probability for evaporation depends on the molecular weight of the individual molecule. In typical situations, the evaporation temperature is high enough that all molecules near the surface can leave the crucible, independent of their weight. There might be however conditions at which the smaller molecules are evaporated, whereas the larger ones remain within the crucible. At an evaporation temperature of 120 °C we reasonably presume that such thermal conditions are present for the polymers used. As a consequence, we believe that the MWD of the evaporated molecules significantly differs from the polymers supplied and a depletion of smaller molecules within the evaporation source causes the time dependence described. In order to obtain a better understanding of this phenomenon, one may take advantage of the experimentally obtained ratio of maximal film thicknesses of 2.6. Here, one may use an iterative approach to shift the MWD_{6000} of the supplied polymer with molecular weight of 6000 g/mol to a reduced average molecular weight M_{red} of the evaporated molecules, such that the integral over this reduced MWD_{red} (grey hatched area in Fig. 7) is 2.6 times higher than the integral over the overlap of MWD_{red} with MWD_{28000}. The ratio of evaporated particles is mainly dependent on the derivation of the molecular weight distributions MWD_{red} and MWD_{28000}, integrated in the range from the lowest

possible value (siloxane monomer: 88 g/mol) to the temperature-dependent value $\overline{M_i}$:

$$\frac{\frac{1}{C_{6000}}\int_{88\mathrm{g/mol}}^{\infty}\left(\frac{P}{M_{6000}}M\exp\left[-\frac{P}{M_{\mathrm{red}}}M\right]\right)\mathrm{d}M}{\frac{1}{C_{28000}}\int_{88\mathrm{g/mol}}^{M_i}\left(\frac{P}{M_{28000}}M\exp\left[-\frac{P}{M_{28000}}M\right]\right)\mathrm{d}M+\frac{1}{C_{6000}}\int_{M_i}^{\infty}\left(\frac{P}{M_{6000}}M\exp\left[-\frac{P}{M_{\mathrm{red}}}M\right]\right)\mathrm{d}M}=2.6. \quad (7)$$

As the number of particles in the reservoir before evaporation is expected to be equal, the MWDs of the supplied polymers are normalized by a factor of $C_{6000}=3750$ and $C_{28000}=17{,}500$. We assumed that the polydispersity P of PDMS corresponded to 1.6 as determined by single-molecule atomic force microscopy [38]. The solution of Eq. (7) leads to an average molecular weight (1500 ± 15) g/mol of the evaporated PDMS with a nominal molecular weight of 6000 g/mol and to (2800 ± 28) g/mol for the evaporated PDMS with a nominal molecular weight of 28,000 g/mol. Here the error bars are given by the ratio of the experimentally determined maximal film thicknesses.Accordingly, the probability of evaporation for molecules above a molecular weight of 7000 g/mol is negligible. We computed that only 6.2% of the polymer with a molecular weight of 6000 g/mol and 2.4% of the polymer with a molecular weight of 28,000 g/mol evaporate at the selected source temperature of 120 °C. These proportions explains the growth rates, which are low compared to the desired rates in the range of 1 μm per hour, and the depletion resulting in maximal film thicknesses of only a few hundreds of nanometers.

These thin films are therefore assumed to consist of molecules with a molecular weight between 88 and about 7000 g/mol. In order to increase the film's stability polymerization should be initiated. Polymerization of elastomer thin films, based on PDMS can be readily reached through hydrosilylation or heat-induced cross-linking reactions involving catalysts [12]. Alternatively the cleavage of the functional groups can also be realized by radicalization with UV light [13]. The radicalization of functional groups was observed with MIR spectroscopy and can be elucidated by assuming two main crosslinking paths. First, the extinction of the 1590 cm^{-1} absorption band indicates that the double bond of the vinyl group was activated under UV-radiation resulting in free highly reactive bonding sites on both sides of the double bond. These are expected to end-link the single chains along these functional groups, either connecting at the free electron on the CH— or the one on the CH_2—side of the vinyl group. Obviously, these connections contribute as an end-linking process to the extension of the polymer chains. Entanglement occurs at chain lengths above 16,000 g/mol as found by Al-Maawali et al. [38]. Thus, this chain length has to be reached to create an entangled network. Second, as observed by Graubner et al. [39,40], we detected a side reaction indicating the radicalization of the methyl (CH_3) side groups either by C—H or even Si—C bond rupture. Under ambient conditions UV-excited oxygen interacts with radicalized Si—C or C—H bonds resulting via side reactions in a cross-linking of the polymer chains by Si—O, Si bonds or $SiCH_2$—CH_2Si bonds to a three-dimensional network. Based on the complete disappearance of the vinyl vibrations we conclude that all the functional end groups were radicalized and linked, whereas for the amount of cross-linked methyl side groups only a qualitative conclusion can be drawn.

The degree of polymerization should be reflected in the mechanical properties of the film. Relying on the model of Mark et al. the elastic modulus for end-linked polymer networks is higher for low molecular weight chains than for networks consisting of high molecular weight polymer chains as the elastic modulus inversely depends on the molecular weight [41]:

$$Y=\frac{C\rho kT}{M_{\mathrm{w}}}. \quad (6)$$

In this equation, $\rho=0.97$ g/cm^{-3} is the density of the PDMS network at $T=298.2$ K, k is the Boltzmann constant and the constant C was determined to be 0.65 [41]. According to this model the elastic modulus of the polymer DMS-V21 with a nominal molecular weight of 6000 g/mol is expected to be 280 kPa. The measured elastic modulus, determined by nanoindentation of a 4-μm, spin-coated, UV-polymerized polymer, was found to be (480.9 ± 0.2) kPa. This result implies that not only chain end-linking throughout the vinyl end groups occurs. Instead, as already proposed by the findings via MIR measurements, also cross-linking via the radicalized methyl-groups along the PDMS chain takes place, which leads to a 1.7 times higher elastic modulus than purely end-linked networks.

The elastic modulus of the MBD-grown DMS-V21 thin film was determined to be (1685.8 ± 1.4) kPa. According to Eq. (6), this value can be related to an average molecular weight of around 1000 g/mol of polymers being evaporated. We note that nanoindentation measurements contain a relative error of approximately 20% introduced by the uncertainty of the cantilever spring constant. This uncertainty is circumvented by comparing the ratios of elastic moduli determined under similar measurement conditions instead of relying on absolute values. Thus we can state that a much higher elastic modulus of the evaporated, UV-polymerized DMS-V21 thin film was found compared to the spin-coated, UV-polymerized thin film. Using the considerations of Mark et al., we estimated the average molecular weight of the evaporated polymer and calculated a value of 1700 g/mol [41]. This conclusion coincides with the considerations on the evaporation above. It should be mentioned that the quantities obtained are rather qualitative, whereas the reasonable hypothesis that the molecules with the lower molecular weight preferentially evaporate perfectly explains the experimental results.For application purposes the most important property is the functionality of the film within the actuator, which can be tested using a cantilever as substrate. At an evaporation temperature of 150 °C a 200 nm-thin DMS-V21 film was grown on an asymmetric cantilever microstructure. The stress-strain transfer is comparable to that of the 4-μm-thick, spin-coated EAP cantilever, but already operates at actuation voltages below 12 V. Therefore, reducing the EAP film thickness is promising for building actuators for medical applications, including artificial muscles.

The maximal curvatures, represented in Fig. 7, correspond to the expected bending moments of $(1.25\pm0.1)\ 10^{-7}$ Nm and $(8.7\pm7.8)\ 10^{-10}$ Nm for the 4 μm-thick polymer at a voltage of 500 V and the 200 nm-thin cantilever actuator at a voltage of 12 V, respectively. Induced by gravity, these curvatures would correspond to bending moments of $(1.03\pm0.05)\times10^{-7}$ Nm and $(2.03\pm0.12)\times10^{-8}$ m for the 4 μm-thick and the 200 nm-thin cantilever actuators according to the calibration measurement, described in Section 3.5. Thus the efficiency, given as the ratio of the bending moments, was found to be (80 ± 8)% for the 4 μm-thick actuator, which is in agreement with the values published in literature for silicone-based DEAs [2]. Using the same approach, we have found a surprisingly high value of approximately 2300% for the 200 nm-thin EAP cantilever. It shows that the 200 nm-thin EAP actuator has more than 23 times higher actuation than expected. We can relate this phenomenon to the inhomogeneity of the polymer film, which contributes to the theoretical bending moment in a quadratic manner.

The breakdown voltage of 60 V/μm for the 200 nm-thin DMS-V21 film, compared to 120 V/μm for the 4 μm-thick Elastosil film, also indicates a significant inhomogeneity of the thermally grown film. We attribute the inhomogeneity more to the incorporated defects during UV-curing in atmosphere than to the MBD process

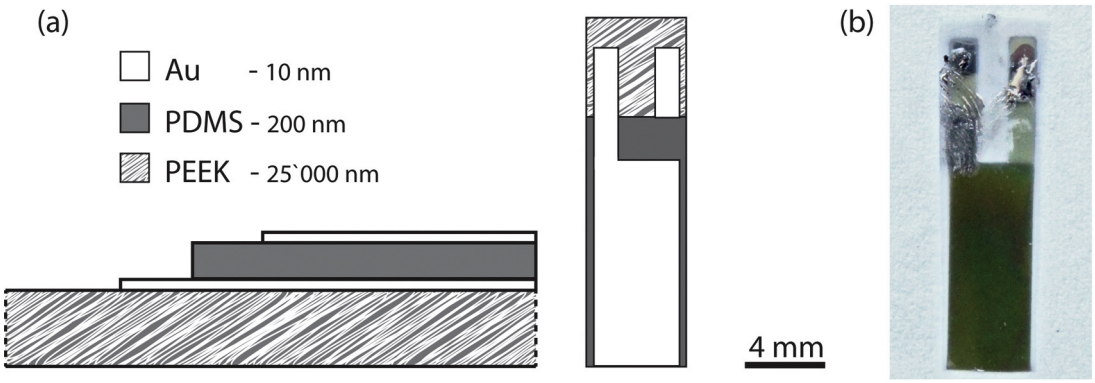

Fig. 8. a) A schematic cross-section and top view of an asymmetric cantilever actuator consisting of a PDMS-film embedded between two 10 nm-thin Au electrodes, placed on a 25 μm-thick PEEK substrate is presented. The shape of the Au electrodes was realized via a mask applied during the sputtering process as described in Section 2.4. b) The photograph of the 200 nm-thin single-layer EAP actuator prototype is shown.

itself. In addition, the UV source used provides an inhomogeneous illumination profile. Enabled through the higher mobility of the low molecular weight PDMS chains this led to a film thickness that is correlated with the irradiation intensity. This hypothesis is proposed based on a visual inspection of the surface, seen on the photograph in Fig. 8, and a statistical thickness measurement with 3D laser microscopy. An average thickness of (210 ± 60) nm was found with ten measurement spots over the active area of the cantilever actuator.

Another contribution to this low breakdown voltage is expected from the diffusion of Au atoms into the polymer film, which was not part of the present study, but is known to have a dominant impact for nanometer-thin elastomer films. A further source of uncertainty is the actual dielectric constant of the evaporated DMS-V21 film. Nevertheless, the breakdown voltage can compete with the values of 70 V/μm obtained for matured silicones such as SVF5 [42]. Assuming that the dielectric properties of the evaporated DMS-V21 thin film are comparable to the Elastosil film, a strain of (5.8 ± 1.5)% was according to Eq. (1) applied to the DMS-V21 network at an operating voltage of 12 V. We expect that the integration of UV-treatment into the high-vacuum environment and an UV-irradiation with a homogenous profile will significantly reduce the defect density and, hence, enhances the breakdown voltage and strain level, respectively.

Regarding the repetition and hysteresis for up to 1500 actuation cycles of such EAP cantilever actuators results, based on micrometer-thick polymer layers, have very recently been published [20], whereas the quantification of these parameters for 200 nm-thin film based EAP actuators is not quantified yet. For the determination of the curvature, however, we repeated the measurement for each data point presented for three times and did not notice any superior hysteresis.

5. Conclusion and Outlook

Molecular beam deposition of vinyl-terminated, siloxane-based polymers has been successfully shown, permitting the fabrication of nanometer-thin polymer films for single-layer EAP actuators. Actuation voltages smaller than 12 V were well below the approved medical limit and illuminate the key advance of these thin-film actuators making them promising candidates for biomimetic artificial muscles. MBD process control was realized by temperature and mass regulation of the utilized polymer. The choice of the polymer chain length allows the growth process as well as the resulting thin film elastic properties to be tailored. We have shown that the chain length defines the network density and therefore the stiffness of the polymer network. Via the polymer molecular weight also the depositions rates and maximal realizable film thicknesses can be regulated. With lower molecular weight polymers higher deposition rates were realized leading to polymer films with a thickness of hundreds of nanometers.

The termination with functional groups at the polymer chain influences the thermal properties of the polymer. The main limitation constitutes the thermal stability of the polymer in use [43]. We proved studies on PDMS with different termination, showing that a vinyl-termination enhances the thermal stability compared to hydride termination [17]. For further improvement, phenyl termination was proposed by Israeli et al., which offers the possibility of using evaporation temperatures above 180 °C and to achieve growth rates faster than 1 μm/h [36]. Combined with a homogeneity of better than 2%, the MBD of polymers allows for a reliable and repeatable growth process for stacked actuators, as needed to reach the desired actuation forces for artificial muscles. Once a multilayer growth process is successfully established, nanometer-thin EAPs will address further applications in the field of biomimetics and robotics with a simplified energy supply as well as a reduced health risk. Proposed as artificial muscles dielectric EPA actuators exhibit strain levels well above 30% within the range of milliseconds response time [4] compared to less than 10% strain within a higher response time of a few seconds for stacked nematic elastomers [44]. Even state-of-the-art, tunable optics, based on relaxor ferroelectric actuators with driving voltages ranging from 40 to 500 V [45], could be replaced by low-voltage EAP actuators.

Acknowledgments

This activity was funded by the Nanotera.ch Initiative, a Collaboration of the Biomaterials Science Center (BMC) of the University of Basel, the Swiss Federal Laboratories for Material Science and Technologies (Empa), the Institute for Surgical Technology and Biomechanics (ISTB), Kantonsspitäler Schaffhausen and Inselspital Bern. The financial support of the Swiss National Science Foundation (project 200021-135496) is gratefully acknowledged. The authors thank Theodor Bühler (University of Applied Sciences Northwestern Switzerland) for the MIR-characterization of the polymer films, and Vitrex Europe for kindly providing the PEEK films.

References

[1] Y. Bar-Cohen, Application of Dielectric EAP Actuators, in: Roy Kornbluh, R. Pelrine (Eds.), Electroactive Polymers (EAP) Actuators as Artificial Muscles – Reality, Potential and Challenges, 2nd ed., SPIE Press, Bellingham, 2004, pp. 475–495.
[2] F. Carpi, D. Rossi, R. Kornbluh, R.P. Pelrine Sommer-Larsen, Dielectric elastomers as high-performance electroactive polymers, in: Dielectric

Elastomers as Electromechanical Transducers, 1st. ed., Elsevier Ltd., Hungary, 2008, pp. 13–21.
[3] R. Pelrine, R. Kornbluh, J. Joseph, R. Heydt, Q. Pei, S. Chiba, High-field deformation of elastomeric dielectrics for actuators, Mater. Sci. Eng. C 11 (2000) 89–100.
[4] R.E. Pelrine, R.D. Kornbluh, J.P. Joseph, Electrostriction of polymer dielectrics with compliant electrodes as a means of actuation, Sens. Actuators A: Phys. 64 (1998) 77–85.
[5] Q.M. Zhang, H. Li, M. Poh, F. Xia, Z.Y. Cheng, H. Xu, et al., An all-organic composite actuator material with a high dielectric constant, Nature 419 (2002) 284–287.
[6] A.E. Daugaard, S.S. Hassouneh, M. Kostrzewske, A.G. Benjenariu, A. Ladegaar Skov, High dielectric permittivity elastomers from well-dispersed expanded graphite in low concentrations, Proc. SPIE 8687 (2013) 868729.
[7] D.B. Hall, P. Underhill, J.M. Torkelson, Spin coating of thin and ultrathin polymer films, Polym. Eng. Sci. 38 (1998) 2039–2045.
[8] G. Kovacs, L. Düring, S. Michel, G. Terrasi, Stacked dielectric elastomer actuator for tensile force transmission, Sens. Actuators A: Phys. 155 (2009) 299–307.
[9] A.V. Rogachev, M.A. Yarmolenko, A.A. Rogachev, D.L. Gorbachev, Specific features of formation and molecular structure of polyaniline-based composite coatings deposited from active gas phase, Russ. J. Appl. Chem. 82 (2009) 1655–1661.
[10] R. Pelrine, R. Kornbluh, Q. Pei, J. Joseph, High-speed electrically actuated elastomers with strain greater than 100%, Science 287 (2000) 836–839.
[11] F.M. Weiss, H. Deyhle, G. Kovacs, B. Müller, Designing micro- and nanostructures for artificial urinary sphincters, Proc. SPIE 8340 (2012) 83400A.
[12] A.G. Wacker Chemie, http://www.wacker.com/cms/de/products/product/product.jsp?product=10461, 1st July 2015.
[13] U. Müller, H.J. Timpe, K.G. Häusler, K. Peters, R. Wagner, Lichtinitiierte polymer- und polymerisationsreaktionen. 36. Mitt.: photovernetzung vinlygruppenhaltiger poly(dimethylsiloxane), Acta Polym. 41 (1990) 54–54-59.
[14] N. Barié, M. Rapp, H.J. Ache, UV crosslinked polysiloxanes as new coating materials for SAW devices with high long-term stability, Sens. Actuators B: Chem. 46 (1998) 97–103.
[15] F.M. Weiss, X. Zhao, P. Thalmann, H. Deyhle, P. Urwyler, G. Kovacs, et al., Measuring the bending of asymmetric planar EAP structures, Proc. SPIE 8687 (2013) 86871X.
[16] P. Urwyler, J. Köser, H. Schift, J. Gobrecht, B. Müller, Nano-mechanical transduction of polymer micro-cantilevers to detect bio-molecular interactions, Biointerphases 7 (2012) 1–8.
[17] Y. Israëli, J. Cavezzan, J. Lacoste, Photo-oxidation of polydimethylsiloxane oils: II-effect of vinyl groups, Polym. Degrad. Stabil. 37 (1992) 201–208.
[18] J.E. Sader, J.W.M. Chon, P. Mulvaney, Calibration of rectangular atomic force microscope cantilevers, Rev. Sci. Instrum. 70 (1999) 3967–3969.
[19] W.C. Oliver, G.M. Pharr, Measurement of hardness and elastic modulus by instrumented indentation: Advances in understanding and refinements to methodology, J. Mater. Res. 19 (2004) 3–20.
[20] T. Töpper, B. Osmani, F.M. Weiss, C. Winterhalter, F. Wohlfender, V.Y.F. Leung, et al., Strain-dependent characterization of electrode and polymer network of electrically activated polymer actuators, Proc. SPIE 9430 (2015) 94300B.
[21] T.C. Hodge, S.A. Bidstrup-Allen, P.A. Kohl, Stresses in thin film metallization, IEEE Trans. Comp. Packag. Manuf. Technol. A 20 (1997) 241–2250.
[22] D.A. Panchuk, S.L. Bazhenov, A.V. Bolshakova, L.M. Yarysheva, A.L. Volynskii, N.F. Bakeev, Correlation between structure and stress-strain characteristics of metallic coatings deposited onto a polymer by the method of ionic plasma sputtering, Polym. Sci. Ser. A 53 (2011) 211–216.
[23] V.K. Pamula, A. Jog, R.B. Fair, Mechanical Property Measurement Of Thin-film Gold Using Thermally Actuated Bimetallic Cantilever Beams, Nanotech, vol. 1, Nano Science and Technology Institute, Duke University, US, 2001, pp. 410–413.
[24] J. Köser, S. Gaiser, B. Müller, Contractile cell forces exerted on rigid substrates, Eur. Cell. Mater. 21 (2011) 479–487.
[25] M. Lallart, C. Richard, P. Sukwisut, L. Petit, D. Guyomar, N. Muensit, Electrostrictive bending actuators: modeling and experimental investigation, Sens. Actuators A: Phys. 179 (2012) 169–177.
[26] F.M. Weiss, T. Töpper, B. Osmani, C. Winterhalter, B. Müller, Impact of electrode preparation on the bending of asymmetric planar electro-active polymer microstructures, Proc. SPIE 9056 (2014) 905607.
[27] V. Racherla, An electromechanical model for characterizing sensing and actuating performance of unimorphs based on plain dielectric polymers, Sens. Actuators A: Phys. 168 (2011) 343–350.
[28] G.G. Stoney, The tension of metallic films deposited by electrolysis, Proc. R. Soc. London Ser. A 82 (1909) 172–175.
[29] R.A. Swalin, Thermodynamics of Solids, John Wiley & Sons, New York, 1972.
[30] P.J. Launer, Infrared Analysis of Organosilicon Compounds: Spectra-structure Correlations, Laboratory for Materials, Inc. Burnt Hills, New York, 1987, pp. 12027.
[31] A.D. Delman, M. Landy, B.B. Simms, Photodecomposition of polymethylsiloxane, J. Polym. Sci. Part A: Polym. Chem. 7 (1969) 3375–3386.
[32] G. Camino, S.M. Lomakin, M. Lazzari, Polydimethylsiloxane thermal degradation Part 1. Kinetic aspects, Polymer 42 (2001) 2395–2402.
[33] S.J. Blanksby, G.B. Ellison, Bond dissociation energies of organic molecules, Acc. Chem. Res. 36 (2003) 255–263.
[34] J.A. Dean, Section 4. Properties of Atoms, Radicals, and Bonds, Lange's Handbook of Chemistry, 15th ed., McGRAWHILL Inc., University of Tennessee, Knoxville, 1999, pp. 441–453.
[35] J.-L.P.Y. Israeli, J. Cavezzan, J. Lacoste, J. Lemaire, Photo-oxidation of polydimethylsiloxane oils: part I-effect of silicon hydride groups, Polym. Degrad. Stabil. 36 (1992) 179–185.
[36] Y. Israeli, J. Lacoste, J. Cavezzan, J. Lemaire, Photooxidation of polydimethylsiloxane oils and resins. IV-Effect of phenyl groups, Polym. Degrad. Stabil. 47 (1995) 357–362.
[37] M. Rogošić, H.J. Mencer, Z. Gomzi, Polydispersity index and molecular weight distributions of polymers, Eur. Polym. J. 32 (1996) 1337–1344.
[38] S. Al-Maawali, J.E. Bemis, B.B. Akhremitchev, R. Leecharoen, B.G. Janesko, G.C. Walker, Study of the polydispersity of grafted poly(dimethylsiloxane) surfaces using single-molecule atomic force microscopy, J. Phys. Chem. B 105 (2001) 3965–3971.
[39] V.-M. Graubner, R. Jordan, O. Nuyken, B. Schnyder, T. Lippert, R. Kötz, et al., Photochemical modification of cross-linked poly(dimethylsiloxane) by irradiation at 172 nm, Macromolecules 37 (2004) 5936–5943.
[40] S.H. Kim, E.A. Cherney, R. Hackam, Effect of Dry Band Arcing on the Surface of Rtv Silicone Rubber Coatings, International Symposium on Electrical Insulation, IEEE, Baltimore MD, USA, 1992, pp. 237–240.
[41] J.E. Mark, J.L. Sullivan, Model networks of end –linked polydimethylsiloxane chains. I. Comparisons between experimental and theoretical values of the elastic modulus and the equilibrium degree of swelling, J. Chem. Phys. 66 (1977) 1006–1011.
[42] C. Löwe, X. Zhang, G. Kovacs, Dielectric elastomers in actuator technology, Adv. Eng. Mater. 7 (2005) 361–367.
[43] P. Kovacik, G. Sforazzini, A.G. Cook, S.M. Willis, P.S. Grant, H.E. Assender, et al., Vacuum-deposited planar heterojunction polymer solar cells, ACS Appl. Mater. Interfaces 3 (2010) 11–15.
[44] C.M. Spillmann, J. Naciri, B.D. Martin, W. Farahat, H. Herr, B.R. Ratna, Stacking nematic elastomers for artificial muscle applications, Sens. Actuators A: Phys. 133 (2007) 500–505.
[45] S.T. Choi, J.O. Kwon, F. Bauer, Multilayered relaxor ferroelectric polymer actuators for low-voltage operation fabricated with an adhesion-mediated film transfer technique, Sens. Actuators A: Phys. 203 (2013) 282–290.

Biographies

Tino Töpper studied at the Albert-Ludwigs University of Freiburg i. Br. and received his diploma degree in physics in 2011. From 2010 to 2011 he prepared his diploma thesis specialized on semiconductor lasers at the Fraunhofer Institute of solid state physics (IAF) in Freiburg where he continued his work after graduation as a research assistant till 2012. Since 2013 he is working towards his Phd degree in physics on the realization of polymer thin films and their characterization by optical means at the Biomaterial Science Center (BMC, University of Basel). As a member of the Nano-Tera founded project "Smartsphincter" he aims for biomedical applications such as implantable low-voltage actuators.

Bekim Osmani did his B.Sc. in Mechanical Engineering and received his M.Sc. in Biomedical Engineering and Robotics at the Swiss Federal Institute of Technology in Zurich (ETHZ) in 2002. He worked from 2002 until 2004 as a scientific assistant at the Institute of Mechatronics at the Zurich University of Applied Sciences in Winterthur. After several years of experience in industry, he is currently working towards his PhD degree in Nanoscience on the fabrication and characterization of dielectric elastomer actuators for medical implants at the University of Basel.

Florian Weiss received his B.Sc. in Chemistry and Molecular Science at the University of Berne Switzerland in 2009, where he continued his studies in Inorganic Chemistry and Materials Science until 2011 when he accomplished his Master degree. After working 6 month in a collaboration project of the University of Bern and BASF he started his PhD at the University of Basel. Currently he is still at the Biomaterials Science Center (BMC, University of Basel) in collaboration with the Empa Dübendorf, Research Center Jülich and the Technical University of Denmark (DTU) to attain his PhD degree in Nanoscience working on MEMS/NEMS mimicking muscles.

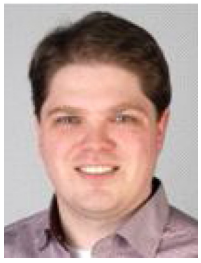

Christian Bippes holds a diploma in Biochemistry from the University of Bayreuth, Germany, and received a PhD from the University of Technology Dresden, Germany, in 2009. From 2009 until 2013 he worked as a post-doc at the University of Technology Dresden, Germany, and ETH Zürich, Switzerland. Currently, he is working as application engineer at Nanosurf AG located in Liestal, Switzerland.

Vanessa Leung holds a B.Sc. (Hons.) in Physics (2001) from Massey University, New Zealand, and a Ph.D. (2006) jointly from the Australian National University, Australia, and the University of Bonn, Germany. This was followed by university research on experiments in atomic, molecular and optical (AMO) physics in Europe and the USA. Since 2012 she has focused on applying physics to technological problems, and doing science at the intersection of academia and industry. As part of a technology initiative between the University of Twente and Philips Lighting in the Netherlands, she used nano-photonics to develop more efficient white LED lighting. She is currently team leader of the Nano-Tera project on Artificial Muscles at the University of Basel.

Bert Müller obtained MSc in Physics and MSc in English from the Dresden University of Technology, and a PhD in experimental physics, University of Hannover, Germany. He was postdoc at Physics Department of Paderborn University, Germany and Feodor Lynen-Fellow at the Physics Department of EPF Lausanne, Switzerland. It followed leading positions within the ETH domain, i.e. at the Physics Department of ETH Zürich, Swiss Institute for Materials Testing and Research, Materials Department and Information Technology and Electrical Engineering Department of ETH Zürich. Since 2001, Bert Müller teaches at the Physics Department of ETH Zürich as 'Privatdozent in Experimentalphysik'. Since 2006 he is Thomas Straumann-Professor for Materials Science in Medicine at the Medical Faculty of the University in Basel. Teaching experiences include the Medical Faculty in Bern (Biomaterials and Materials Science), Dental School of the University of Basel (Dental Materials and Technologies) and Science Faculty (Nanosciences and Surface Science). Currently, he is director of the Biomaterials Science Center and leads a research team of almost 30 scientists from several disciplines. The research activities include high-resolution X-ray imaging, biomaterials science and engineering, and artificial muscles. He is author of more than 200 scientific publications including patents.